Available online at www.sciencedirect.com
SCIENCE DIRECT
Catalysis Today 110 (2005) 191–198
CATALYSIS TODAY
www.elsevier.com/locate/cattod

Low temperature decomposition of nitrous oxide over Fe/ZSM-5: Modelling of the dynamic behaviour

Lioubov Kiwi-Minsker *, Dmitri A. Bulushev, Albert Renken

Laboratoire de Génie de la Réaction Chimique, Ecole Polytechnique Fédérale, CH-1015 Lausanne, Switzerland

Available online 2 November 2005

Abstract

The kinetics of N_2O decomposition to gaseous nitrogen and oxygen over HZSM-5 catalysts with low content of iron (<400 ppm) under transient and steady-state conditions was investigated in the temperature range of 250–380 °C. The catalysts were prepared from the HZSM-5 with Fe in the framework upon steaming at 550 °C followed by thermal activation in He at 1050 °C. The N_2O decomposition began at 280 °C. The reaction kinetics was first order towards N_2O during the transient period, and of zero order under steady-state conditions. The increase of the reaction rate with time (autocatalytic behaviour) was observed up to the steady state. This increase was assigned to the catalysis by adsorbed NO formed slowly on the zeolite surface from N_2O. The formation of NO was confirmed by temperature-programmed desorption at temperatures >360 °C. The amount of surface NO during the transient increases with the reaction temperature, the reaction time, and the N_2O concentration in the gas phase up to a maximum value. The maximum amount of surface NO was found to be independent on the temperature and N_2O concentration in the gas phase. This leads to a first-order N_2O decomposition during the transient period, and to a zero-order under steady state. A kinetic model is proposed for the autocatalytic reaction. The simulated concentration–time profiles were consistent with the experimental data under transient as well as under steady-state conditions giving a proof for the kinetic model suggested in this study.

Keywords: Fe-containing HZSM-5; N_2O decomposition; Transient response method; Temperature-programmed desorption; Kinetic modelling

1. Introduction

ZSM-5 zeolites doped with iron are a growing focus of interest due to high catalytic activity in industrial applications. This catalyst is used in the N_2O decomposition to O_2 and N_2 [1–9]. The observed activity strongly depends on the catalyst preparation, composition (Si/Al and Fe/Al ratios) and zeolite activation [10–21]. In our previous publications [1,22], we reported that traces of iron (<1000 ppm) in isomorphously substituted HZSM-5 upon steaming and/or high temperature calcinations in He renders the catalyst highly active towards N_2O decompositions at low temperatures (280 °C ≤ T ≤ 380 °C). The catalyst activity is known to be sensitive to the presence of other gases in the stream like H_2O, CO, NO, hydrocarbons, etc. Different research groups have observed that NO accelerates N_2O decomposition [23–29]. The activated catalysts lose their activity for the low temperature N_2O decomposition in the presence of water vapours. The N_2O decomposition starts in this case only above 400 °C indicating the importance of the state of iron for catalysis.

Evidence for the reaction mechanism involving the formation of surface oxygen atom, $(O)_{Fe}$, from N_2O by reaction (1) have been reported in recent studies:

$$N_2O + (\,)_{Fe} \rightarrow N_2 + (O)_{Fe} \quad (1)$$

Two neighbouring $(O)_{Fe}$ can recombine forming O_2 by reaction (2):

$$2(O)_{Fe} \rightarrow O_2 + 2(\,)_{Fe} \quad (2)$$

The latter step of oxygen desorption is accepted to be the rate limiting step for the N_2O decomposition. This reaction is accelerated by the presence of NO. We recently reported the first experimental evidence of the slow NO formation on the catalyst surface from N_2O leading to autocatalytic kinetic behaviour [1].

The objective of the present work is to study the transient and steady-state kinetics of N_2O decomposition and to suggest

* Corresponding author. Tel.: +41 21 693 31 82; fax: +41 21 693 61 90.
E-mail address: lioubov.kiwi-minsker@epfl.ch (L. Kiwi-Minsker).

0920-5861/$ – see front matter © 2005 Elsevier B.V. All rights reserved.
doi:10.1016/j.cattod.2005.09.039

a kinetic model consistent with experiments. We applied in this study the transient response method and temperature-programmed reaction to monitor the dynamics of the N_2O interaction with the catalyst. The isomorphously substituted zeolites with low content of iron (<400 ppm) (H(Fe)ZSM-5) were employed in order to avoid the formation of Fe oxide nano-particles upon activation.

2. Experimental

2.1. Catalyst preparation

The ZSM-5 zeolites used in the present study were prepared by hydrothermal synthesis described elsewhere [30]. HZSM-5_{200} and HZSM-5_{350} have Si/Al = 42 and the iron concentration of 200 and 350 ppm, respectively. Typically, tetraethylorthosilicate (TEOS; Fluka, 98%) was added to an aqueous solution of tetrapropyl-ammonium hydroxide (TPAOH; Fluka, 20% in water) used as a template, $NaAlO_2$ (Riedel-de Haën, Na_2O 40–45%, Al_2O_3 50–56%). The molar ratios of the components were TEOS:TPAOH:$NaAlO_2$:H_2O = 0.8:0.1:0.016–0.032:33. The mixture was stirred for 3 h at room temperature, and the clear gel obtained was transferred to a stainless-steel autoclave lined with PTFE and kept at 180 °C for 2 days. The product was filtered, washed with deionised water and calcined in air at 550 °C for 12 h. The zeolite was then converted into the H-form by an exchange with a NH_4NO_3 aqueous solution (0.5 M) and subsequent calcination at 550 °C for 3 h.

The catalysts were activated by steaming (H_2O partial pressure of 0.3 bar, He flow rate—50 ml/min) at 823 K for 4 h and also by heating at 1050 °C in He (50 ml/min) for 1 h.

2.2. Catalyst characterization

The chemical composition of the catalysts was determined by atomic absorption spectroscopy (AAS) via a Shimadzu AA-6650 spectrometer. The samples were dissolved in boiling aqua regia containing several drops of HF.

X-ray diffraction (XRD) patterns of catalysts were obtained on a Siemens D500 diffractometer with Cu Kα monochromatic radiation (λ = 1.5406 Å).

The active sites concentration measurements, reactivity of deposited oxygen and temperature-programmed desorption/reaction (TPD/TPR) experiments were performed in a Micromeritics AutoChem 2910 analyser provided with a quartz plug-flow reactor. A ThermoStar 200 (Pfeiffer Vacuum) mass-spectrometer was used to control the composition of gas phase. Calibrations were carried out with gas mixtures of known compositions. The catalysts (1.04–1.09 g) after pre-treatments were cooled down in He to the temperature of the transient response study (250–380 °C). The latter was performed by a quick switch of the He flow to the stream consisting of: 2 vol.% N_2O/2 vol.% Ar/96 vol.% He at a flow rate 20 ml (STP)/min. N_2O reacts with the catalyst resulting in the formation of gaseous nitrogen and atomic oxygen bound by the catalyst according to the reaction (1). The amount of active sites was calculated by integration of the nitrogen peak area.

2.3. Reaction dynamics study

Reaction dynamics study was also performed in a Micromeritics AutoChem 2910 analyser. The gases were supplied by Carbogas, Switzerland (purities > 99.998%). The NO_x content in N_2O was below 2 ppm. The following peaks were monitored simultaneously by the mass-spectrometer 4 (He), 18 (H_2O), 28 (N_2, N_2O), 30 (NO, N_2O), 32 (O_2), 40 (Ar), 44 (N_2O) and 46 (NO_2) *m/e*. The set-up as well as a fused silica capillary connected to the mass-spectrometer were heated up to 110 °C. Sometimes, an NO_x detector (EcoPhysics CLD 822) with a sensitivity of >10 ppm of NO_x was used to identify the nitrogen oxides during the N_2O interaction with the catalyst. The amount of a catalyst placed in a quartz plug-flow reactor was equal to 0.5–1.0 g. Before the runs, the activated catalysts were pre-treated in He (50 ml/min) at 1050 °C for 1 h, then cooled down to the selected temperature.

In the transient experiments normally a mixture 2 vol.% N_2O/2 vol.% Ar in He was used unless it was desired to vary the N_2O concentration. For these experiments, the mixtures containing 1.3 and 0.7 vol.% of N_2O were prepared by dilution of the original mixture with He. Argon was always added as an inert tracer gas. The same flow rate was used for all gas compositions (20 ml (STP)/min). For temperature-programmed reaction studies, the catalysts were heated in the same reaction mixture with a ramp programmed at 10 °C/min.

3. Results and discussion

3.1. Transient responses at different temperatures

The transient response curves of N_2O, Ar (tracer), N_2 and O_2 within the first 300 s after the switch in the reactor inlet from He to the reaction mixture at 250 °C are shown in Fig. 1. Nitrous oxide evolution is delayed with respect to Ar (inert tracer) due to products formation and also due to reversible N_2O adsorption on the catalyst surface. The N_2 concentration passes a maximum indicating the surface oxygen loading in accordance

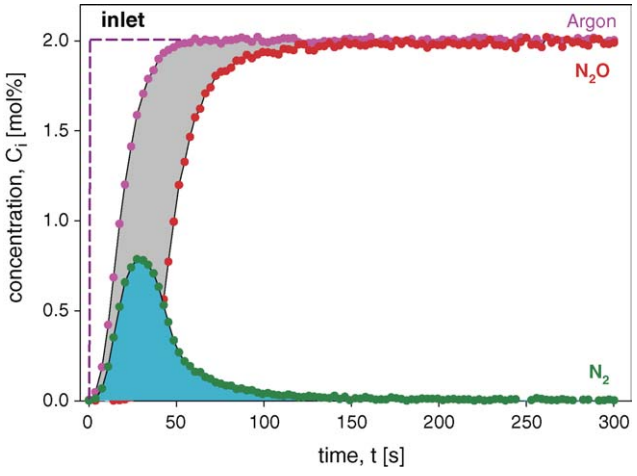

Fig. 1. Transient response curves obtained after introduction of the 2 vol.% N_2O/2 vol.% Ar rest He mixture on the HZSM-5_{350Fe} catalyst at 250 °C after the standard pre-treatment. Points—experimental data; lines—simulation results.

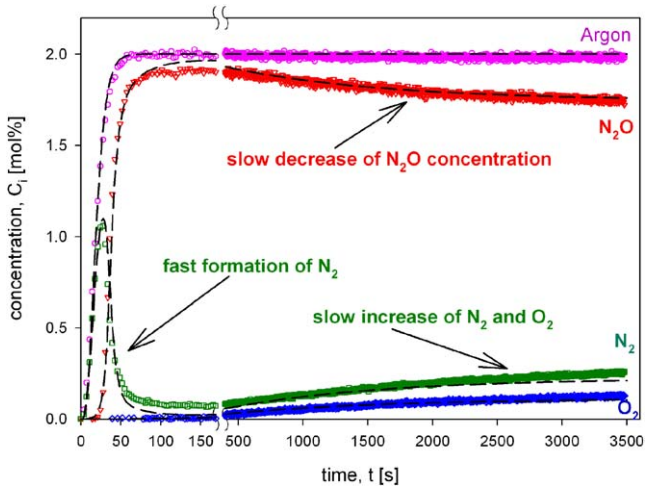

Fig. 2. Transient response curves obtained after introduction of the 2 vol.% N_2O/2 vol.% Ar rest He mixture on the HZSM-5_{350Fe} catalyst at 300 °C after the standard pre-treatment. Points—experimental data; lines—simulation results.

with the reaction step (1). No oxygen evolution was observed at this temperature. Integrating the area between Ar and N_2O curves after subtraction of the N_2 curve gives the quantity of nitrous oxide molecules adsorbed. The total amount of oxygen atoms adsorbed on Fe sites was determined by the integration of the N_2 peak surface and gives the total amount of sites involved in the reaction (1). This assignment is formal: N_2 appears as an asymmetric peak with a tailing up to 200 s. This shape of the N_2 response could not be described by the rate of the reaction (1) only. The response pattern suggests also another source of N_2 formation.

The transient response experiment with HZSM-5_{350} at 300 °C is presented in Fig. 2 showing the formation of N_2 and O_2. The N_2 concentration also first passes via a sharp maximum indicating the surface oxygen loading. The initial reaction period is followed by the slow increase of the N_2 and O_2 concentrations in stoichiometric ratio until reaching steady state after ∼1 h. The same response was observed at temperatures >300 °C (Fig. 3), but the steady-state conversion was much higher and attained more rapidly. At 380 °C the conversion of 100% was observed after 100 s (see Fig. 4).

It is important to mention that the amount of O_2 determined by TPD after cooling the sample in the reaction mixture was the same for all experiments in the selected temperature range. This observation indicates a complete coverage of active Fe sites by atomic oxygen at low temperatures.

3.2. Kinetics of N_2O decomposition under steady-state conditions

Different authors reported that the kinetics of the N_2O decomposition is of first order towards nitrous oxide and the rate can be written as:

$$r_{N_2O} = k_{app} P_{N_2O} \quad (3)$$

It is important to note that the majority of the studies have been carried out at temperatures >400 °C. Under these conditions, the reaction rate is very high and the steady state is reached within few seconds. This is not the case at temperatures 280–380 °C used in this study. It is seen from the transient response curves (Figs. 1–4) that the rate increases in time due to autocatalysis. Depending on the reaction temperature, it takes up to 2 h to attain the reaction rate corresponding to the steady state.

To determine the reaction order in N_2O under steady-state conditions, its decomposition was studied at 310 °C. Steady state was attained after ca. 1 h, and then three consecutive changes of the reactant mixture composition were performed keeping the total gas flow rate constant. The inlet N_2O concentration was changed from 2.0 to 1.3 and to 0.7%. Finally, the concentration was adjusted again to 2% to prove the reproducibility of the experiment and the catalyst stability. The results are presented in Fig. 5 showing no influence of N_2O inlet concentration on the O_2 and N_2 (not shown) outlet concentrations. This means that the rate of N_2O decomposition is independent on its inlet concentration, indicating zero order in N_2O under steady-state conditions.

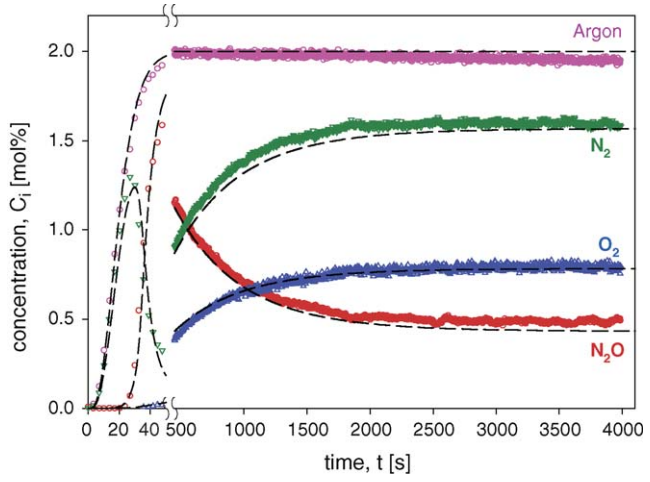

Fig. 3. Transient response curves obtained after introduction of the 2 vol.% N_2O/2 vol.% Ar rest He mixture on the HZSM-5_{350Fe} catalyst at 330 °C after the standard pre-treatment. Points—experimental data; lines—simulation results.

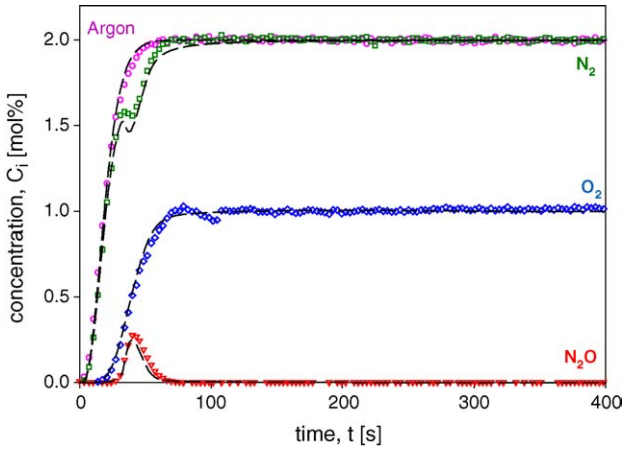

Fig. 4. Transient response curves obtained after introduction of the 2 vol.% N_2O/2 vol.% Ar rest He mixture on the HZSM-5_{350Fe} catalyst at 380 °C after the standard pre-treatment. Points—experimental data; lines—simulation results.

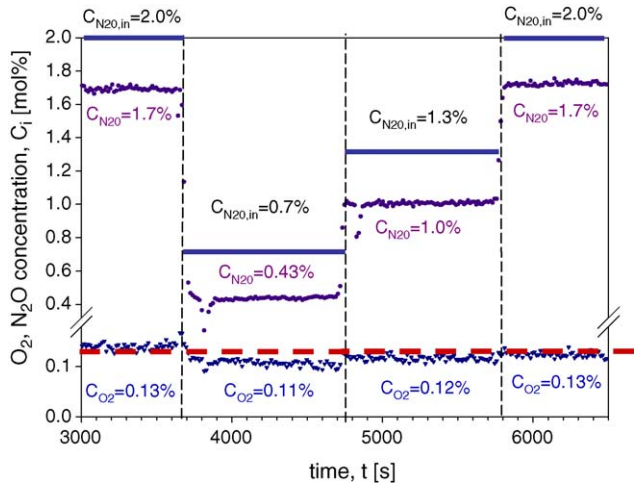

Fig. 5. O_2 outlet and N_2O inlet and outlet concentrations monitored during N_2O decomposition over the HZSM-5_{350Fe} catalyst at 310 °C under steady-state conditions.

3.3. Temperature-programmed reaction

Temperature-programmed reaction is often used to study the reaction kinetics to obtain orders of the reaction and activation energy. TPR was performed with different N_2O concentration (0.7–2.0%) with the ramp set at 10 K/min, following the sample pre-treatment for 5 min at 250 °C in the reaction mixture. The results are presented in Fig. 6 showing N_2O conversion (X, %) versus temperature. It is seen that the decomposition of N_2O to O_2 and N_2 begins above 280 °C. Moreover, no dependence of conversion on the inlet N_2O concentration was observed. This indicates the first order in N_2O since the conversion does not depend on the reactant concentration:

$$X = 1 - \exp(-k \cdot \tau)$$

where k is the rate constant according to Arrhenius law and τ is the mean residence time, which was kept constant in all experiments.

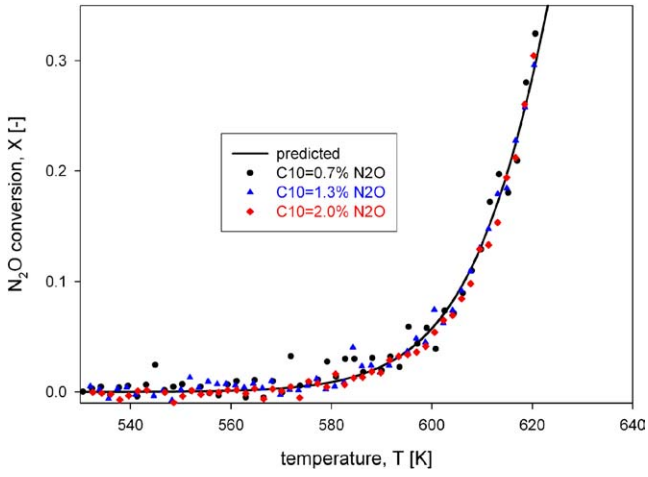

Fig. 6. N_2O conversion as a function of temperature (temperature-programmed reaction) obtained over the HZSM-5_{350Fe} catalyst with different N_2O concentrations of: 0.7, 1.3 and 2.0 vol.% in He after 5 min pre-treatment at 250 °C.

First-order N_2O decomposition was observed in a number of studies and reported recently by Wood et al. using TPR method [8].

The discrepancy (the first order observed by TPR and zero order at constant temperature of 310 °C under steady-state conditions) may arise from the fact that the TPR can only be used for kinetic studies if the catalyst reaches steady state at each temperature during the temperature increase. The latter condition is not satisfied, at least at temperatures <400 °C as seen from the reaction dynamics (Figs. 1–4).

3.4. Temperature-programmed desorption

In our previous publication [1], we assigned the autocatalytic behaviour (the increase of the reaction rate with time) during N_2O decomposition at low temperatures to the catalysis by adsorbed NO formed slowly on the catalyst surface from N_2O. The catalytic effect of the adsorbed NO was also confirmed by transient experiments with pulse addition of NO in the N_2O stream during its decomposition. In this case, the steady-state reaction rate was attained immediately after the NO pulse [1]. Therefore, we can relate the change of the observed reaction order towards N_2O when passing from transient to the steady-state conditions, to the increasing surface concentration of NO during the transient period. In order to prove this assumption, the amount of adsorbed NO was measured by TPD performed after 5 min exposure of the catalyst at 250 °C to the reaction mixture with different concentrations of N_2O (between 0.7 and 2.0%). The results are presented in Fig. 7a showing a higher peak for the NO desorbed with the increasing N_2O gas-phase concentration. Integration of the TPD peak area allows to determine the total amount of NO formed during the same time. Fig. 7b demonstrates that this amount increases proportionally with the concentration of N_2O. This is the reason for the observed first-order reaction kinetics of the N_2O decomposition under the transient conditions observed by TPR (see Fig. 6).

The amount of adsorbed NO attains a constant value when the catalyst reaches a steady state. This amount was found to be independent on the reaction temperature and equal to 2.5×10^{-3} mol/kg. The same amount of NO was desorbed from the catalyst upon exposure to NO (0.5% NO in He) at 250 °C followed by the reactor purge by He. These results suggest that the formation of adsorbed NO on the zeolite surface at temperatures up to 360 °C is slowly attaining a maximum, $C^{surface}_{NO,max}$, which corresponds to a complete coverage by NO ($\theta_{NO} = 1$).

An argument could be put forward that NO is not formed from N_2O, but it may be present as an impurity in the N_2O and would accumulate slowly on the zeolite surface. In this case, the formation of surface NO would be the result of NO adsorption step, but not of chemical reaction. The transient curves would then not depend on the temperature. Also, the catalytic effect would decrease with temperature since the adsorption equilibrium of gases diminishes with temperature. In Fig. 8, the transient concentration of oxygen in the gas phase referred

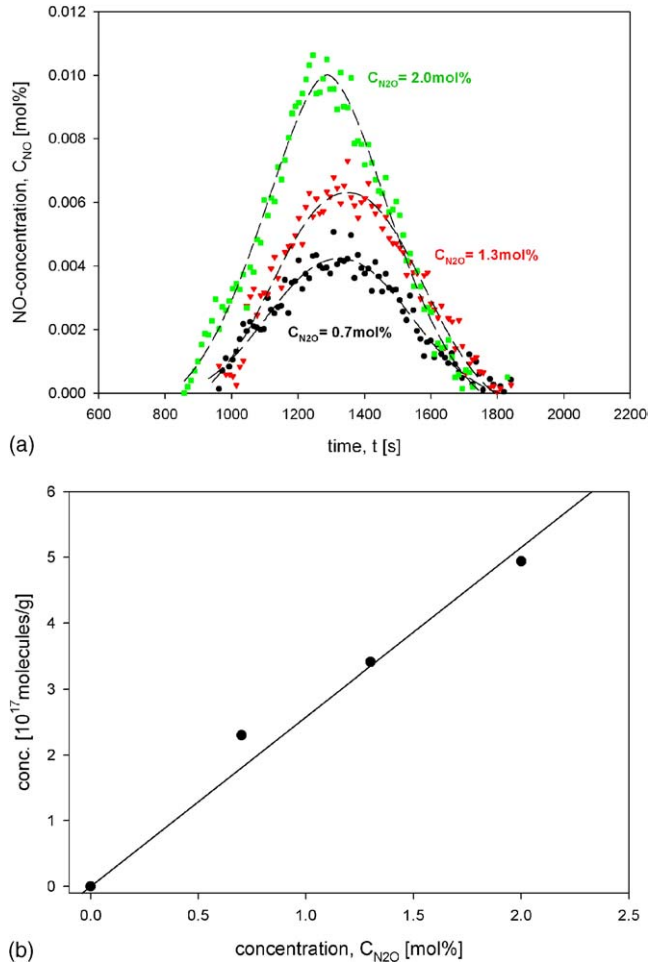

Fig. 7. (a) NO concentration profiles during TPD runs in the mixture with 0.7, 1.3 and 2.0 vol.% N_2O in He after the exposure of HZSM-5_{350Fe} for 5 min at 250 °C. (b) The amount of NO desorbed in TPD runs (see (a)) as a function of N_2O concentration in the gas phase.

to its steady-state value is plotted as a function of time for different temperatures. It is seen that the increase of the reaction rate is more marked for higher temperatures confirming the chemical interaction of N_2O with the surface leading to adsorbed NO.

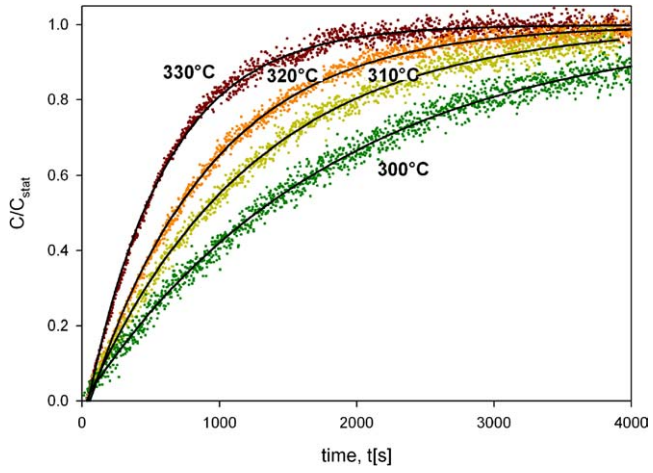

Fig. 8. Transient concentration of oxygen in the gas phase referred to its steady-state value as a function of time for different temperatures. Points—experimental data; lines—simulation results.

3.5. Kinetic scheme of N_2O decomposition at low temperatures over H(Fe)ZSM-5

The experimental data and an analysis of alternative steps for the low temperature decomposition of N_2O over H(Fe)ZSM-5 allows to suggest the following reaction kinetic scheme:

$$N_2O_{gas} \leftrightarrow N_2O_{ad}\ (\text{reversible adsorption}) \quad \text{instantaneous} \tag{4}$$

$$N_2O_{ad} + (\,)_{Fe} \rightarrow N_2 + (O)_{Fe}\ (\text{deposition of oxygen}) \quad \text{fast} \tag{5}$$

$$N_2O_{ad} + [\,]' \rightarrow [NO]' + N_2\ (\text{formation of surface NO}) \quad \text{relatively fast} \tag{6}$$

$$[NO]' \rightarrow [NO]\ (\text{accumulation of catalytic NO}) \quad \text{slow} \tag{7}$$

$$[NO] + 2(O)_{Fe} \rightarrow O_2 + 2(\,)_{Fe} + [NO]\,\}\ (\text{catalytic formation of } O_2) \quad \text{relatively fast} \tag{8}$$

$$2(O)_{Fe} \rightarrow O_2 + 2(\,)_{Fe}\ (\text{non-catalytic formation of } O_2) \quad \text{slow} \tag{9}$$

At 250 °C only the steps presented by Eqs. (4)–(7) seem to take place. The first step corresponds to the reversible adsorption of N_2O followed by the surface atomic oxygen loading with the release of molecular nitrogen (step (5)). The $[NO]'$ is formed in the step (6) giving also N_2 in the gas phase. Evidence for the relatively fast step (6) comes from the pattern of N_2 response: it appears as an asymmetric peak with a tailing up to 200 s and could not be described by the rate of the step (5) only. The response pattern suggests another source of N_2 besides the deposition of atomic oxygen. Therefore, we suggested a relatively fast formation of surface NO as described by the step (6). Another reason for the tailing of the N_2 peak may come from the heterogeneity of the iron sites involved in the oxygen loading on surface presented by Eq. (5).

The step (6) in the kinetic scheme is not an elementary reaction and may proceed in two steps:

$$N_2O_{ad} + (O)_{Fe} \rightarrow NO_{ad} + (\,)_{Fe}$$

$$N_2O_{ad} + (O)_{Fe} \rightarrow N_2 + (\,)_{Fe}$$

Since the observed acceleration of stoichiometric N_2O decomposition is a slow process at temperatures $T \leq 330$ °C, a slow transformation of the $[NO]'$ sites to the sites [NO] was suggested and described by the step (7).

The detailed mechanism of the NO formation on the catalyst surface is still not clear. But NO species is accumulated on sites different from those involved in the atomic oxygen loading, $(\,)_{Fe}$. This was confirmed by separate experiments pulsing NO into the reaction mixture, which did not lead to any reaction inhibition as could be expected in the case of competitive adsorption on the same sites [1]. Non competitive adsorption of NO and $(O)_{Fe}$ is indicated also by the TPD after the reaction runs during the same time but at different temperatures <380 °C: the NO amount desorbed increased with temperature, but the amount of O_2 was found independent on the amount of NO adsorbed.

The observed overall N_2O interaction with FeZSM-5 at low temperature (<280 °C) can be stated as:

$$N_2O_{ad} + (\,)_{Fe} \rightarrow (O)_{Fe} + NO_{ad} + N_2$$

where NO_{ad} refers to different forms of NO species on the zeolite surface including [NO]′ and [NO].

The step (8) of atomic oxygen recombination catalyzed by [NO] is not an elementary reaction since the collision of three molecules is unlikely as an elementary step. It may proceed probably via the formation of surface [NO_2]:

$$[NO] + (O)_{Fe} \rightarrow [NO_2] + (\,)_{Fe}$$

$$[NO_2] + (O)_{Fe} \rightarrow O_2 + [NO] + (\,)_{Fe}$$

The sequence of these reactions is kinetically equivalent to the step (8), since the surface coverage by atomic oxygen is $\theta_O = 1$ at low temperatures (<380 °C).

The rates of reactions (4)–(9) can be expressed by Eqs. (4a)–(9a). Instantaneous equilibrium is assumed for the adsorption of N_2O (Eq. (4a)). The rate coefficients k_i include the maximum surface concentration of active sites for NO and atomic oxygen, $C^{surface}_{O,max}$ and $C^{surface}_{NO,max}$, respectively.

$$C^{surface}_{N_2O} = K_{ad} C^{gas}_{N_2O} \tag{4a}$$

$$r_1 = k_1 \cdot C^{surface}_{N_2O} \cdot (1 - \theta_O) \tag{5a}$$

$$r_2 = k_2 \cdot C^{surface}_{N_2O} \cdot (1 - \theta'_{NO}) \tag{6a}$$

$$r_s = k_s \cdot \theta'_{NO} \cdot (1 - \theta_{NO}) \tag{7a}$$

$$\begin{aligned} r_3 &= k_3 \cdot \theta_{NO}\ (\theta_O = 1) \quad \text{(in transient period)} \\ r_{3ss} &= k'_3 \cdot C^{surface}_{NO,max} \quad \text{(in steady state)} \end{aligned} \tag{8a}$$

$$r_4 = k_4 \theta^2_O \tag{9a}$$

The dynamic behaviour of the reactor was simulated using the tanks in series model combined with the kinetic models shown in Eqs. (4)–(9). The resulting material balances for the jst tank of the different species in the gas phase are summarized in the following equations:

$$\frac{dC_{N_2O}(j)}{dt} = \frac{C_{N_2O}(j-1) - C_{N_2O}(j)}{\tau_j (1 + K_{ad} C_{cat})} - (r_1(j) + r_2(j)) \cdot C_{cat} \tag{10}$$

$$\frac{dC_{N_2}(j)}{dt} = \frac{C_{N_2}(j-1) - C_{N_2}(j)}{\tau_j} + (r_1(j) + 0.5 \cdot r_2(j)) \cdot C_{cat} \tag{11}$$

$$\frac{dC_{O_2}(j)}{dt} = \frac{C_{O_2}(j-1) - C_{O_2}(j)}{\tau_j} + (r_3(j) + 2 \cdot r_4(j)) \cdot C_{cat} \tag{12}$$

with $C_{cat} = \frac{m_{cat}}{V}$ as a catalyst concentration [kg/m^3] and $\tau_j = \tau/N$ as a mean residence time in one tank.

The surface coverage by the reactants in each stage is given in Eqs. (13)–(15) supposing instantaneous equilibrium for N_2O and irreversible adsorption of atomic oxygen and NO.

$$\frac{d\theta_O(j)}{dt} = \frac{r_1(j) - r_3(j) - r_4(j)}{C^{surface}_{O,max}} \tag{13}$$

$$\frac{d\theta'_{NO}(j)}{dt} = \frac{r_2(j) - r_s(j)}{(C')^{surface}_{NO,max}} \tag{14}$$

$$\frac{d\theta_{NO}(j)}{dt} = \frac{r_s(j)}{C^{surface}_{NO,max}} \tag{15}$$

The number of the tanks in series was estimated from the residence time distribution obtained from the transient response measurements with argon as tracer (Figs. 1–4). The response on the stepwise increase of the argon concentration could be described satisfactorily with $N = 5$ tanks for all experiments.

The differential equations (10)–(15) were solved simultaneously by numerical integration using a variable step algorithm of the commercially available ‘‘Madonna’’ software [31].

The parameters used for the kinetic modelling were estimated independently based on the following experimental results:

- the mean residence time in the reactor and the number of tanks (tanks in series model) by the tracer response curves: $\tau = 22$ s; $N = 5$;
- the maximum surface concentration of atomic oxygen by the amount of nitrogen formed at $T \leq 250$ °C (Fig. 1): $C^{surface}_{O,max} = 5 \times 10^{-3}$ mol/kg;
- the maximum surface concentration of NO from TPD experiment by integrating the peak of NO appeared at $T > 360$ °C: $C^{surface}_{NO,max} = 2.5 \times 10^{-3}$ mol/kg;
- the equilibrium constant at different temperatures taking into account the time delay between Ar and N_2O responses (Fig. 1);
- the rate constant of stoichiometric decomposition of N_2O (k_3) from steady-state experiments at different temperatures (Fig. 5);
- the non-catalytic formation of O_2 (Eqs. (9) and (9a)) was found to be negligible in the temperature range investigated.

The other parameters of the kinetic model were estimated simultaneously by fitting the dependence of concentration on time curves under transient conditions. The optimal set of

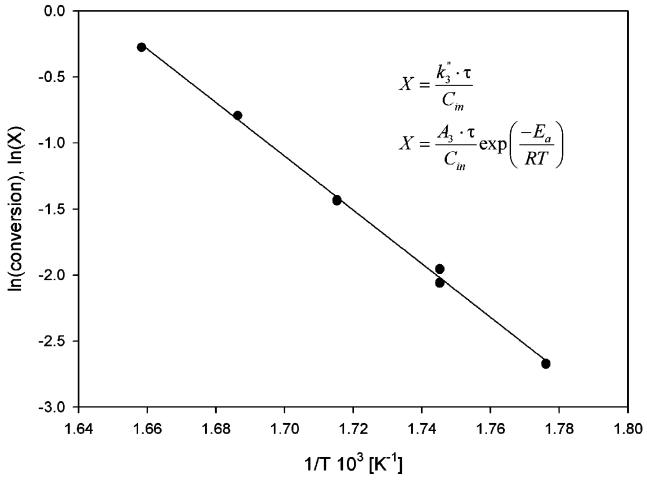

Fig. 9. Temperature dependence of N_2O conversion at steady state assuming zero order in N_2O.

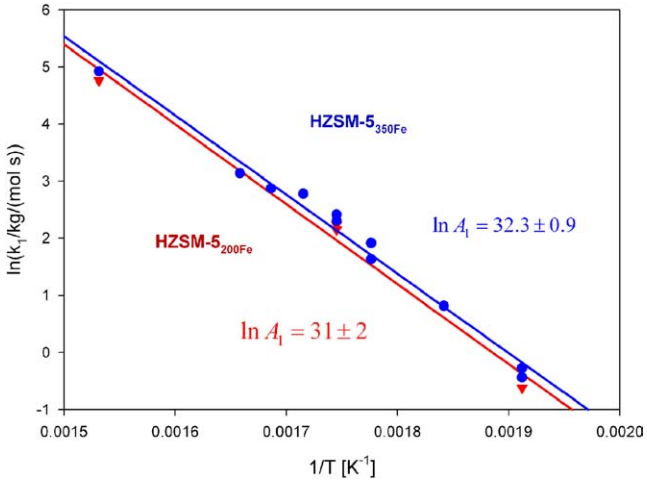

Fig. 11. Temperature dependence of the rate coefficient k_1, of atomic oxygen deposition on the surface (Eqs. (5) and (5a)).

parameters was obtained using the build-in optimization routine of the ''Madonna'' software [31].

The results predicted by the model are displayed in Figs. 1–4 as dashed lines show that the model was consistent with experimental data.

The N_2O conversion obtained in the steady state from 280 to 380 °C is shown in the form of an Arrhenius plot in Fig. 9. From the slope of the straight line an apparent activation energy for the N_2O decomposition of $E_a = 169.4 \pm 5.5$ kJ/mol is calculated. This value agrees with those published by Panov et al. [32]: 155 kJ/mol; Bell and coworkers: 179 kJ/mol (2002 [9]) and 185 kJ/mol (2004 [8]); Perez-Ramirez et al. [28]: 161 kJ/mol; Zhu et al. [10]: 136–213 kJ/mol.

The adsorption enthalpy of N_2O on the catalyst (Eqs. (4) and (4a)) is estimated from the temperature dependence of the equilibrium constant K_{ad} as presented in Fig. 10. A value of $\Delta H_{ad} = -53 \pm 2$ kJ/mol is obtained. Fig. 11 shows an Arrhenius plot for the fast deposition of atomic oxygen (step (5) in the reaction scheme, Eqs. (5) and (5a)) on two zeolites with 200 and 350 ppm of Fe. For both catalysts, an apparent activation energy of 116 ± 5 kJ/mol is obtained. As the number of active sites for the catalyst HZSM-5_{200} is lower compared to HZSM-5_{350}, the apparent pre-exponential factors A_1 also differ. Bell and coworkers [8] found an activation energy of 70 kJ/mol for the deposition of atomic oxygen on H(Fe)ZSM-5. The authors supposed a direct interaction between the catalysts with N_2O from the gas phase, neglecting the preliminary adsorption step. Therefore, the observed by them activation energy includes the adsorption enthalpy of N_2O: $E_{obs} = E_a + \Delta H_{ad}$; $E_a = 70 + 53 = 123$ kJ/mol being close to the one obtained in the present study 116 ± 5 kJ/mol.

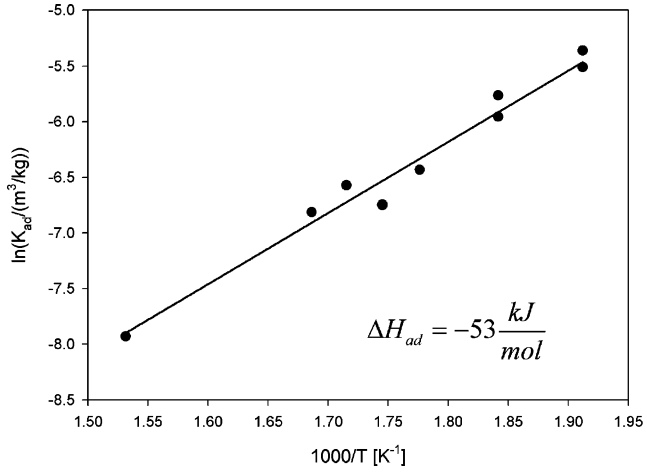

Fig. 10. Adsorption equilibrium of N_2O as function of temperature.

4. Conclusions

The kinetics of N_2O decomposition to O_2 and N_2 at low temperatures 250–380 °C was investigated under transient and steady-state conditions. The aim was to identify the rate parameters for the elementary steps and to develop a kinetic model. The zeolites were isomorphously substituted H(Fe)ZSM-5 with low Fe content (<400 ppm), activated by steaming at 550 °C and thermal treatment in He at 1050 °C. From the transient response experiments, it was established that the reaction involves reversible adsorption of N_2O with the enthalpy $\Delta H_{ad} = -53$ kJ/mol. N_2 is formed by the interaction of adsorbed N_2O with a vacant Fe site: $N_2O_{ad} + (\,)_{Fe} \rightarrow N_2 + (O)_{Fe}$. This reaction step has activation energy of 116 ± 5 kJ/mol. Oxygen desorption occurs by association of two $(O)_{Fe}$ atoms and is catalyzed by NO adsorbed on the sites different from $(\,)_{Fe}$. Autocatalytic effect was observed and assigned to the surface NO. The latter is produced from N_2O and slowly accumulated on the zeolite surface. The amount of adsorbed NO was proportional to the N_2O concentration in the gas phase during the transient period and attained the same maximum value at steady state independently on the reaction temperature (below 380 °C) and the N_2O concentration. This leads to the observed first order in N_2O during the transient period and to zero order in N_2O in steady-state regime. The simulated concentration-time profiles were consistent with the experimental data during transient as well as in steady-state

regimes providing credence for the suggested kinetic model. The apparent activation energy for the steady-state decomposition of N_2O to O_2 and N_2 being ~170 kJ/mol, agrees with the results reported in literature.

Acknowledgment

Financial support from the Swiss National Science Foundation is gratefully acknowledged.

References

[1] D.A. Bulushev, L. Kiwi-Minsker, A. Renken, J. Catal. 222 (2004) 389.
[2] K.A. Dubkov, N.S. Ovanesyan, A.A. Shteinman, E.V. Starokon, G.I. Panov, J. Catal. 207 (2002) 341.
[3] A. Heyden, B. Peters, A.T. Bell, F.J. Keil, J. Phys. Chem. B 109 (2005) 1857.
[4] F. Kapteijn, G. Mul, G. Marban, J. Rodriguez Mirasol, J.A. Moulijn, Decomposition of nitrous oxide over ZSM-5 catalysts, in: 11th International Congress on Catalysis—40th Anniversary, Pts A and B, 1996, p. 641.
[5] J. Perez-Ramirez, F. Kapteijn, A. Bruckner, J. Catal. 218 (2003) 234.
[6] J. Perez-Ramirez, F. Kapteijn, G. Mul, X.D. Xu, J.A. Moulijn, Catal. Today 76 (2002) 55.
[7] G.D. Pirngruber, J. Catal. 219 (2003) 456.
[8] B.R. Wood, J.A. Reimer, A.T. Bell, M.T. Janicke, K.C. Ott, J. Catal. 224 (2004) 148.
[9] B.R. Wood, J.A. Reimer, A.G. Bell, J. Catal. 209 (2002) 151.
[10] Q. Zhu, B.L. Mojet, R.A.J. Janssen, E.J.M. Hensen, J. van Grondelle, P. Magusin, R.A. van Santen, Catal. Lett. 81 (2002) 205.
[11] Q. Zhu, R.M. van Teeffelen, R.A. van Santen, E.J.M. Hensen, J. Catal. 221 (2004) 575.
[12] K.Q. Sun, H.D. Zhang, H. Xia, Y.X. Lian, Y. Li, Z.C. Feng, P.L. Ying, C. Li, Chem. Commun. (2004) 2480.
[13] G.D. Pirngruber, M. Luechinger, P.K. Roy, A. Cecchetto, P. Smirniotis, J. Catal. 224 (2004) 429.
[14] J. Perez-Ramirez, E.V. Kondratenko, Chem. Commun. (2003) 2152.
[15] J. Perez-Ramirez, F. Kapteijn, G. Mul, J.A. Moulijn, Appl. Catal. B Environ. 35 (2002) 227.
[16] J. Perez-Ramirez, F. Kapteijn, J.C. Groen, A. Domenech, G. Mul, J.A. Moulijn, J. Catal. 214 (2003) 33.
[17] J. Perez-Ramirez, A. Gallardo-Llamas, Appl. Catal. A Gen. 279 (2005) 117.
[18] P. Marturano, L. Drozdova, A. Kogelbauer, R. Prins, J. Catal. 192 (2000) 236.
[19] M.S. Kumar, M. Schwidder, W. Grunert, A. Bruckner, J. Catal. 227 (2004) 384.
[20] E.J.M. Hensen, Q. Zhu, M. Hendrix, A.R. Overweg, P.J. Kooyman, M.V. Sychev, R.A. van Santen, J. Catal. 221 (2004) 560.
[21] E.J.M. Hensen, Q. Zhu, R.A. van Santen, J. Catal. 220 (2003) 260.
[22] L. Kiwi-Minsker, D. Bulushev, A. Renken, Catal. Today 91–92 (2004) 165.
[23] C.M. Sang, B.H. Kim, C.R.F. Lund, J. Phys. Chem. B 109 (2005) 2295.
[24] T. Nobukawa, M. Yoshida, K. Okumura, K. Tomishige, K. Kunimori, J. Catal. 229 (2005) 374.
[25] M.N.D. Boutarbouch, J.M.G. Cortes, M.S. El-Begrani, C.S.M. de Lecea, J. Perez-Ramirez, Appl. Catal. B Environ. 54 (2004) 115.
[26] J. Perez-Ramirez, F. Kapteijn, Chem. Commun. 4 (2003) 333.
[27] J. Perez-Ramirez, G. Mul, F. Kapteijn, J.A. Moulijn, Kinet. Catal. 44 (2003) 639.
[28] J. Perez-Ramirez, F. Kapteijn, G. Mul, J.A. Moulijn, J. Catal. 208 (2002) 211.
[29] G. Mul, J. Perez-Ramirez, F. Kapteijn, J.A. Moulijn, Catal. Lett. 77 (2001) 7.
[30] L. Kiwi-Minsker, D.A. Bulushev, A. Renken, J. Catal. 219 (2003) 273.
[31] R. Macey, G. Oster, Madonna 7.0, University of California, Berkeley, 1999.
[32] G.I. Panov, V.I. Sobolev, A.S. Kharitonov, J. Mol. Catal. 61 (1990) 85.